Preparation of Poly(*N*-isopropylacrylamide)-Monolayer-Protected Gold Clusters: Synthesis Methods, Core Size, and Thickness of Monolayer

Jun Shan,[†] Markus Nuopponen,[†] Hua Jiang,[‡] Esko Kauppinen,[‡] and Heikki Tenhu*[,†]

Laboratory of Polymer Chemistry, University of Helsinki, PB 55, FIN-00014 HY, Finland, and VTT Processes, Materials and Chemicals, PB 1602, FIN-02044 VTT, Finland

Received February 28, 2003; Revised Manuscript Received April 17, 2003

ABSTRACT: The preparation of poly(*N*-isopropylacrylamide)-monolayer-protected clusters (PNIPAM-MPC) of gold nanoparticles was carried out in a homogeneous phase using three methods, in which three types of PNIPAM ligands were employed. The first type was comprised of PNIPAMs with narrow molar mass distributions, synthesized by reversible addition−fragmentation chain transfer (RAFT) polymerization and thus bearing a dithiobenzoate at the chain end. These polymers were used directly to passivate the gold nanoparticles upon the Schiffrin reaction in a one-pot synthesis. The second type of ligand was derived from the first one through hydrazinolysis, and they therefore contained a thiol end group. The third type of ligand was PNIPAMs obtained through conventional radical polymerization, postmodified to contain thiol end groups. The PNIPAM-MPCs were characterized by high-resolution transmission electron microscopy, UV−vis spectroscopy, and dynamic light scattering. The one-pot synthesis utilizing the ligands of the first type turned out to be a simple and facile method compared with the other two ways, with which the size of the gold nanoparticles can be easily manipulated mainly by adjusting the molar ratios of PNIPAM/$HAuCl_4$. PNIPAM is a more efficient ligand to stabilize the gold nanoparticles in water and in organic solvents than alkanethiols. The surface density of PNIPAM chains ranged from 1.8 to 2.5 chain/nm^2, which is much lower than that typical for alkanethiols. The thickness of a PNIPAM monolayer bound to the gold core is somewhat larger than the size of the random coil of the corresponding free PNIPAM in aqueous solution, which suggests that the conformation of a PNIPAM chain bound to the gold core is extended.

Introduction

Monolayer-protected clusters (MPC) of metal nanoparticles constitute a rapidly emerging field of chemical research due to the very specific electronic, optoelectronic, and catalytic properties of the clusters derived from the quantum-scale dimension.[1−5] MPC is a core−shell nanocomposite composed of a metal core and a shell ranging from small organic compounds to macromolecules. The organic shell can be further functionalized in various ways. Among the metal cores, particularly gold, silver and copper have been the major focus because of their unique optical properties[6,7] for the design of, for example, optoelectronic analytical devices.[8,9] In particular, since a reliable way to prepare gold nanoparticles passivated by alkanethiols was first demonstrated by Schiffrin,[10] much effort has been made on the synthesis and monolayer functionalization,[11−17] the control of the size and monodispersity of the gold core, and the core structure[18−20] and on the properties of MPCs[21−23] in order to develop new building blocks for optical, electronic, and biomedical applications.

Recently, a method using thiolated polymers as ligands to protect gold nanoparticles has been developed,[24,25] which shows that the thiolated polymer ligands are more efficient than alkanethiols in preparing small sized gold nanoparticles and stabilizing the particles in solutions as well as in increasing their thermoresistance. Importantly, the properties and potentials of MPCs may be extended when using polymer ligands with different architectures to stabilize gold nanoparticles. In general, two strategies, "grafting-from" and "grafting-to", can be utilized to prepare gold nanoparticles with well-defined covalently bound polymer monolayers. The "grafting-from" strategy is based on the surface-initiated polymerization, by which better uniformity and controlled thickness of the polymer shell on the surface of various solids are possible to obtain if living polymerization techniques are applied.[26−29] In the case of gold nanoparticles, end-functionalized monolayers, regarded as macroinitiators, may be used to initiate living/controlled polymerization directly on the surface of the particles. Several researchers reported that the "grafting-from" strategy could construct a highly dense polymer brush on the surface of gold nanoparticles. Jordan et al.[30] used the surface-initiated living cationic polymerization to prepare a nanocomposite where the gold core was coated with an amphiphilic shell with a well-defined hydrophilic/lipophilic balance. Using surface-initiated atom transfer radical polymerization (ATRP), gold nanoparticles coated with poly(methyl methacrylate)[31,32] as well as with poly(*n*-butyl acrylate)[33] were recently prepared. We previously reported the synthesis of gold nanoparticles grafted with a thermoresponsive polymer by surface-induced reversible addition−fragmentation chain transfer (RAFT) polymerization.[34]

In the "grafting-to" strategy, polymers end-capped with a thiol group or containing a disulfide unit have been used instead of small alkanethiol ligands upon the Schiffrin reaction to prepare directly the polymer MPCs of gold nanoparticles. Teranishi et al.[24] used poly(mercaptomethylstyrene-*co*-*N*-vinyl-2-pyrrolidone) to stabilize gold nanoparticles. Murray et al.[25] reported a monolayer-protected gold cluster based on a monolayer

[†] University of Helsinki.
[‡] VTT Processes, Materials and Chemicals.
* Corresponding author: tel +358-9-19150334; fax +358-9-19150330; e-mail Heikki.Tenhu@helsinki.fi.

10.1021/ma034265k CCC: $25.00
Published on Web 05/14/2003

of α-methoxy-ω-mercapto-poly(ethylene glycol) (PEG-SH, molar mass 5000). Corbierre et al.[35] reported gold nanoparticles covalently passivated with a thiol end-capped polystyrene prepared by anionic polymerization. Mangeney et al.[36] reported the grafting of gold clusters with nonionic hydrophilic polymers containing disulfide group anchors. The resulting polymeric monolayer was further derivatized and used for the specific recognition of analytes.

The "grafting-to" strategy is an especially useful synthetic route to prepare polymer stabilized gold clusters, if combined with a living polymerization technique. This is because the polymer ligands can be well-defined prior to being employed to prepare gold nanoparticles. Particularly, this strategy is promising when a polymer from a RAFT reaction bearing dithioester end groups is directly used as a passivant. The dithioester end groups are reduced to thiols when adding a reducant to the mixed solution of $HAuCl_4$ and the RAFT polymer, and the gold cores are passivated with the resulting thiols. Just recently, a paper was published using this concept, in which Lowe et al.[37] reported the synthesis of gold nanoparticles stabilized by anionic, cationic, neutral, and zwitterionic (co)-polymers.

We studied the change in the surface plasmon band of the gold clusters upon coating with PNIPAM.[34] To further investigate the optical and optoelectronic properties as well as the solution properties as functions of the size and PNIPAM coating of gold clusters, herein, we employed the "grafting-to" strategy to prepare PNIPAM-MPCs of gold nanoparticles by three methods. Three types of PNIPAMs were used: (i) PNIPAMs bearing dithiobenzoate end groups, from RAFT polymerizations; (ii) PNIPAM end-capped with a thiol group obtained through hydrazinolysis of the former PNIPAM; (iii) thiol-functionalized PNIPAM, obtained through a conventional radical polymerization and following modification. These three methods will be compared and discussed in terms of the size and the size distribution of the resulting gold nanoparticles.

Experimental Section

Chemicals. *N*-Isopropylacrylamide (NIPA, Polyscience Inc.) was recrystallized twice from benzene. Styrene (Aldrich) was distilled under reduced pressure prior to use. Hydrogen tetrachloroaureate(III) hydrate ($HAuCl_4 \cdot xH_2O$, Au content 52%, Fluka). 1.0 M solution of lithium triethylborohydride ($LiB(C_2H_5)_3H$) in THF. 4,4′-Azobis(4-cyanopentanoic acid) (ACPA, Fluka) was used as received. 2,2′-Azobis(isobutyronitrile) (AIBN, Fluka) was recrystallized from methanol. Tetrahydrofuran (THF) (Lab-Scan, HPLC) used for the synthesis of gold nanoparticles was dried by refluxing over calcium hydride and freshly distilled prior to use. Dioxane (Lab-Scan, Analytical Ac.) was distilled before use. Anhydrous methanol was obtained by mixing methanol (J.T. Baker, HPLC) with sodium sulfate. Hydrazine hydrate ($H_2N-NH_2 \cdot H_2O$, 80%), sodium methoxide solution in methanol (~30%, 5.4 M, Fluka), 1-ethyl-3-(3-(dimethylamino)propyl) carbodiimide hydrochloride (EDAC), benzyl chloride, elemental sulfur, α-methylstyrene (Aldrich), cysteamine hydrochloride, iodine, starch soluble (Merck), and alumina (Merck) were used as received. All other solvents with high quality, acetone, ethanol, diethyl ether, benzene, and carbon tetrachloride, were used as received. The water used for all the measurements was purified and deionized in an Elgastat UHQ-PS purification system.

1. Synthesis of the Cumyl- and Cpa-RAFT-PNIPAMs by RAFT Polymerization. Two types of PNIPAMs were synthesized by the RAFT polymerization starting from the preparation of two types of RAFT agents, i.e., the 2-phenylprop-2-yl dithiobenzoate (cumyl-RAFT) and 4-cyanopentanoic acid dithiobenzoate (cpa-RAFT). Therefore, two PNIPAM samples were named the cumyl- and cpa-RAFT-PNIPAMs, respectively. The cumyl-RAFT-PNIPAM is water-insoluble due to the hydrophobic end groups, whereas the cpa-RAFT-PNIPAM bearing a carboxylic group is water-soluble as well. The synthetic routes of RAFT agents[38,39] and two RAFT-PNIPAMs were described earlier.[40] Their molar masses and polydispersities are 4722, 1.10 and 5418, 1.13, respectively, measured by SEC.

2. Synthesis and Modification of Carboxyl-Terminated PNIPAM (PNIPAM-COOH). Synthesis of PNIPAM-COOH. PNIPAM-COOH was synthesized by conventional free radical polymerization. In the three-neck round-bottom flask, the recrystallized NIPAM monomer (0.1 mol) was dissolved in 100 mL of ethanol and mixed with the initiator ACPA (2.0 mmol). The solution was kept in the ice−water bath and degassed by nitrogen over half an hour and then transferred to an oil bath at 70 °C and polymerized for 20 h. The reaction mixture was concentrated by a rotary evaporator. The crude product was dissolved in 50 mL of acetone, precipitated in 200 mL of diethyl ether, and separated using centrifugation. Repeating the procedure twice, the white product of PNIPAM-COOH was dried in a vacuum at 45 °C over 48 h. The molar mass of PNIPAM-COOH is $M_n = 10\,884$, PDI = 1.52, measured by SEC.

Modification of PNIPAM-COOH and Determination of the Thiol Group Content of PNIPAM-SH. PNIPAM-COOH was modified into PNIPAM-SH through the formation of an amide bond between the primary amino group of cysteamine and the carboxylic acid end group of PNIPAM. The carboxylic acid moieties of PNIPAM were activated by the addition of EDAC. The thiol content of the PNIPAM-SH sample was determined by iodometric titration. The procedures of the modification and the titration were described in detail.[41,42] The thiol group content of the PNIPAM-SH is 17.6 μmol/g.

3. Preparation of PNIPAM-Monolayer-Protected Clusters of Gold Nanoparticles (PNIPAM-MPCs) in the Homogeneous Phase via Three Methods. Three methods, according to the modification steps of PNIPAM sample, have been used to prepare PNIPAM-MPCs always in a homogeneous THF phase.[43]

Method 1: One-Step Way To Prepare PNIPAM-MPCs. Three PNIPAM-MPCs were prepared in a one-pot reaction using cumyl- and cpa-RAFT-PNIPAM with different feed ratios (Scheme 1). The concentration of $HAuCl_4 \cdot xH_2O$ was always kept at 0.1 mmol and the molar ratio of $LiB(C_2H_5)_3H/HAuCl_4 \cdot xH_2O$ over 10/1. The details of the preparation of cpa-PNIPAM-MPC (1/5) are described as an example below. To a vigorously stirred yellow solution of 0.1 mmol (37.9 mg) of $HAuCl_4 \cdot xH_2O$ in 10 mL of anhydrous THF was added 0.02 mmol (108 mg) of pink cpa-RAFT-PNIPAM in 10 mL of anhydrous THF (the molar ratio cpa-RAFT-PNIPAM/$HAuCl_4 \cdot xH_2O$ = 1/5). The mixture was stirred for 20 min in an ice bath. Then, 1.2 mL of 1.0 M solution of $LiB(C_2H_5)_3H$ in THF was added dropwise for 2 min to the vigorously stirred solution. The mixture solution turned immediately brown with a little gas evolution and was stirred in an ice bath for a further 4 h. The resulting mixture was first separated by a centrifuge at 15 000 rpm; only a small amount of precipitate was observed at the bottom of centrifuge tube, and the supernatant was collected. THF in the supernatant was removed with a rotary evaporator. The brown crude product was dissolved in 50 mL of deionized water, the pH of the aqueous solution was adjusted to 6−7 with 0.1 M HCl, and the solution was purified by ultrafiltration using a membrane with molar mass cutoff 10 000 and deionized water as eluent. Finally, the concentrated aqueous solution was frozen and lyophilized. The color of cpa-PNIPAM-MPC(1/5) was brown-purple. The other two PNIPAM-MPCs, cpa-PNIPAM-MPC(1/12) and cumyl-PNIPAM-MPC(1/12), both with purple color, were prepared and purified using the same procedure except for the feed ratios, cpa- or cumyl-RAFT-PNIPAM/$HAuCl_4 \cdot xH_2O$ = 1/12.

Method 2: Two-Step Way To Prepare PNIPAM-MPCs. As is shown in Scheme 1, the two-step way includes the

Scheme 1. Schematic Representation of Three Ways To Prepare PNIPAM-MPCs

One-step way:

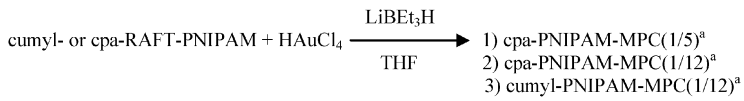

Two-step way:

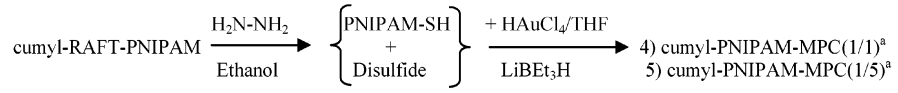

Three-step way:

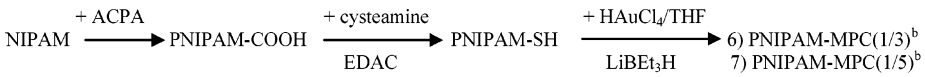

[a] The ratios 1/1, 1/5, and 1/12 denote the molar ratios of cumyl- or cpa-RAFT-PNIPAM/ $HAuCl_4$ used in the preparation of gold nanoparticles. [b]The ratios 1/3 and 1/5 denote the molar ratios of thiol group of PNIPAM/ $HAuCl_4$ used in the preparation of gold nanoparticles.

hydrolysis of cumyl-RAFT-PNIPAM into cumyl-PNIPAM-SH as the first step and the preparation of cumyl-PNIPAM-MPCs (1/1 and 1/5) as the second step.

Hydrazinolysis of Cumyl-PNIPAM-RAFT. 3.55 g (0.75 mmol) of cumyl-RAFT-PNIPAM was dissolved in 100 mL of ethanol in a two-neck round-bottom flask with stirring, and a pink solution was formed. 1.0 mL (over 20-fold of the equimolar amount of cumyl-RAFT-PNIPAM) of hydrazine was injected dropwise with a syringe; the hydrazinolysis started immediately along with the rapid fading of the pink color of the solution and was allowed to continue for 1 h at room temperature under nitrogen. The progress of the reaction was followed by UV−vis spectrometry until the absorbance maximum of dithiobenzoate group at 498.6 nm disappeared. The pH of the resulting mixture was adjusted to 3 using 0.1 M HCl, and then the solvent was removed with a rotary evaporator. The crude product was dissolved in THF and precipitated in diethyl ether. After three repetitive purifications, a white precipitate of cumyl-PNIPAM-SH was attained.

Preparation of Cumyl-PNIPAM-MPCs (1/1 and 1/5). The cumyl-PNIPAM-MPC (1/1 and 1/5) were then prepared using the cumyl-PNIPAM-SH by the same procedure as described in the "one-step way", except for the different ratios, i.e., molar ratios 1/1 and 1/5 of cumyl-PNIPAM-SH/$HAuCl_4 \cdot xH_2O$, respectively. The cumyl-PNIPAM-MPC(1/1) sample is completely brown while the cumyl-PNIPAM-MPC(1/5) is brown-purple.

Method 3. Three-Step Way To Prepare PNIPAM-MPCs. In this method, the synthesis and modification of PNIPAM-COOH as well as the determination of thiol content of PNIPAM-SH were described in detail above. PNIPAM-MPC (1/3 and 1/5) were prepared using the same procedure as described in the "one-step way" with molar ratios 1/3 and 1/5 of PNIPAM-SH/$HAuCl_4 \cdot xH_2O$, and both of the MPCs were purple.

Instrumentation and Characterization. Spectroscopy. UV−vis absorption spectra (400−800 nm) were recorded on a Shimadzu UV-1601PC spectrophotometer from the methanol solutions of PNIPAM-MPCs at 20 °C. ^1H NMR spectroscopy measurements were conducted with a 200 MHz Varian Gemini 2000 spectrometer using deuterated chloroform as a solvent. FT-IR spectra of the RAFT-PNIPAM-SH and RAFT-PNIPAMs were recorded with a Spectrum 2000 (Perkin-Elmer). However, the thiol end group of the PNIPAM chain could not be detected.

High-Resolution Transmission Electron Microscopy (HRTEM). HRTEM images were obtained with a Philips CM200FEG, working at an accelerating voltage of 200 kV. The point-to-point resolution was 0.24 nm. Images were recorded by a GATAN slow scan CCD camera. Samples were prepared by drop-casting one drop of the appropriately diluted cluster solution in methanol onto the holey carbon film on a copper grid (S147-4, 400 mesh Cu, Agar Scientific Ltd.) and dried in air. The size distribution of gold nanoparticles was measured from the enlarged photographs of the TEM images for at least 80−140 individual gold core images.

Thermogravimetric Analysis (TGA). The amount of PNIPAM ligand on the gold core surface was determined by a Mettler Toledo TGA 850 in a flowing nitrogen atmosphere. The temperature was increased from 20 to 800 °C at a rate of 10 °C/min.

Dynamic Light Scattering (DLS). DLS measurements were conducted at 20 °C with a Brookhaven Instruments BI-200SM goniometer and a BI-9000AT digital correlator. The light source was a Lexel 85 argon laser (514.5 nm, power range 30−150 mW and 90°). The time correlation functions were analyzed with a Laplace inversion program (CONTIN). All of the solutions in methanol and in deionized water for polymers and clusters were filtered through Millipore membranes (0.45 μm pore size). The concentrations of aqueous solutions of MPCs were 0.136, 0.0170, and 0.0165 mg/mL for the cumyl-PNIPAM-MPCs (1/1, 1/5, and 1/12), respectively, and 0.0160 and 0.0135 mg/mL for cpa-PNIPAM-MPC (1/5 and 1/12), respectively. The concentrations of cumyl and cpa-RAFT-PNIPAMs were 3.0 mg/mL in methanol and 1.0 mg/mL in deionized water.

Size Exclusion Chromatography (SEC). The molar mass and the polydispersity of each PNIPAM sample were determined with a Waters liquid chromatography system equipped with a Waters 2410 differential refractometer as a detector. Three Styragel columns (HR2, HR4, and HR6) were used in series. A 50 μL aliquot of the sample was injected, and THF was used as an eluent with a flow rate of 0.8 mL/min at 30 °C. The calibration was carried out with polystyrene standards (Showa Denko). It is well-known that the determination of the molar mass of PNIPAM is problematic. However, with low molar mass polymers ($MW < 5 \times 10^4$) the method seems to be reliable. This was confirmed by estimating the molar masses by ^1H NMR spectroscopy.

Results and Discussion

Characterization of the Gold Cores and the Comparison of Three Methods of Synthesis. The HRTEM images, and corresponding size distributions of three PNIPAM-MPCs prepared by the one-step way, are shown in Figure 1. The mean diameters of the gold nanoparticles are listed in Table 1. The PNIPAM-MPCs are well-separated and have reasonably narrow size distributions. The size of the gold core decreases when increasing the molar ratio of RAFT-PNIPAM/$HAuCl_4$, which is in good accordance with the other previous studies on the alkanethiols as ligands.[11,14,18] Only the amount of RAFT-PNIPAM was changed whereas the $HAuCl_4$ concentration was kept constant in all recipes.

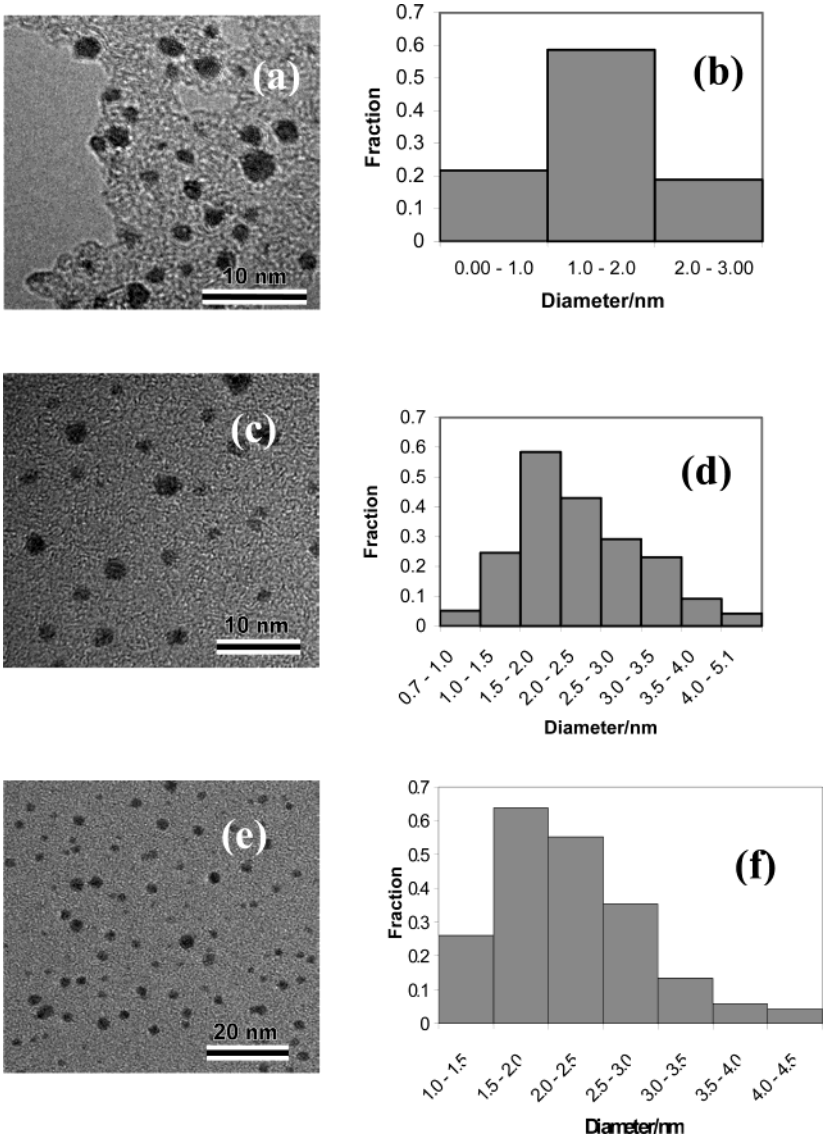

Figure 1. HRTEM images and corresponding size distributions of three MPCs prepared by the one-step method: (a, b) for the cpa-PNIPAM-MPC (1/5); (c, d) for the cpa-PNIPAM-MPC (1/12); (e, f) for the cumyl-PNIPAM-MPC (1/12).

Table 1. Characterizations of Gold Cores

PNIPAM-MPC	method	mean diam of Au core[a] (nm)	no. Au atoms[b]/ shape[b]	no. surface atoms[b]/ area[b](nm^2)
(1) cumyl-PNIPAM-MPC(1/1)	two-step	1.3 ± 0.4	79/TO$^+$	60/8.3
(2) cumyl-PNIPAM-MPC(1/5)	two-step	2.0 ± 0.8	314/TO$^+$	174/19
(3) cumyl-PNIPAM-MPC(1/12)	one-step	2.2 ± 0.8	459/TO$^+$	234/24
(4) cpa-PNIPAM-MPC(1/5)	one-step	1.5 ± 0.5	116/TO$^-$ 78/11	
(5) cpa-PNIPAM-MPC(1/12)	one-step	2.3 ± 0.8	459/TO$^+$	234/24
(6) PNIPAM-MPC(1/3)	three-step	5	4794/TO$^+$	1230/108
(7) PNIPAM-MPC(1/5)	three-step	6	6266/TO	1472/129

[a] Determined by HRTEM. [b] The number of Au atoms per core, shape of Au cluster, number of surface atoms, and surface area for each Au cluster are calculated as in refs 11 and 14. The shape model of the Au cluster was advocated by Whetten in refs 19 and 20. TO = ideal truncoctahedron (all sides equal); TO$^+$ = truncoctahedron in which ($0 < n - m \leq 4$), where n id the number of atoms between (111) facets and m is the number of atoms between (111) and (100) facets; TO− = truncoctahetron in which ($-4 \leq n - m < 0$, $m > 1$). Note that owing to the presence of discernible populations in the core size histograms (see Figures 1−3), the shape model and the number of Au atoms per core are all derived from the average.

It may be concluded that the PNIPAM ligand is a more efficient passivant of the growth of the gold core than alkanethiols because the size of the gold core in this investigation is smaller than that passivated by similar amount of an alkanethiol. Murray reported the same point in his paper[25] where a thiolated poly(ethylene glycol) with molar mass 5000 was utilized to passivate the growth of the gold core. One PEG-S-MPC sample with average core diameter 2.8 ± 1 nm was prepared with a molar ratio 1/12 of PEG-SH/$HAuCl_4$ in a modified Schiffrin reaction (in two phases). In the present case, the mean sizes of the gold cores for the cumyl- and cpa-PNIPAM-MPCs (1/12) are respectively 2.2 ± 0.8 and 2.3 ± 0.8 nm, all smaller than that of PEG-S-MPC (1/12), which means that the RAFT-PNIPAMs used in the one-step way are at least as good passivants as PEG-SH.

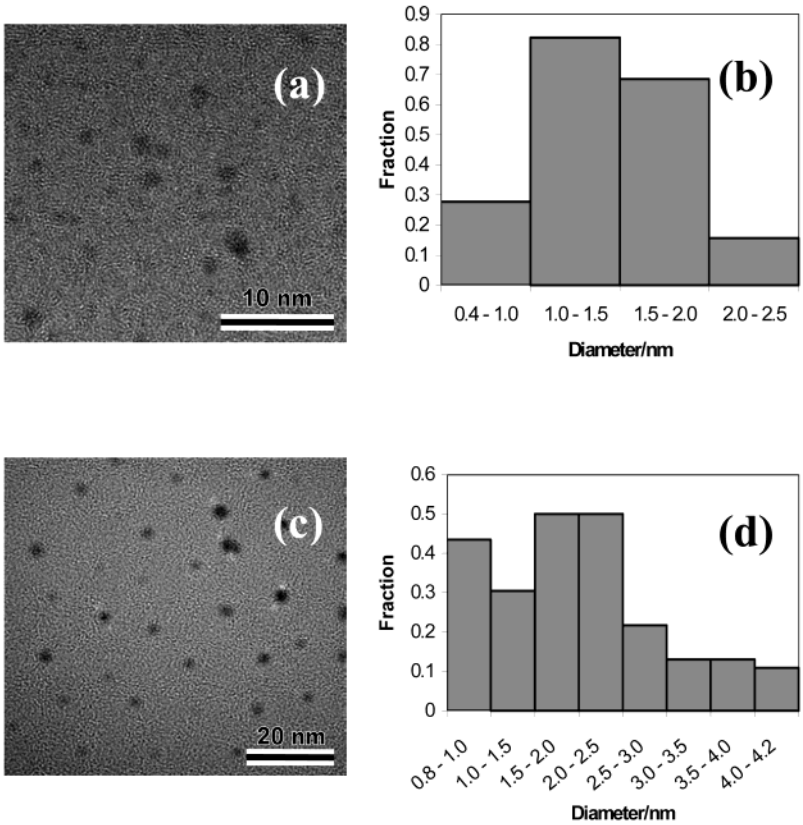

Figure 2. HRTEM images and corresponding size distributions of two MPCs prepared by the two-step method: (a, b) for the cumyl-PNIPAM-MPC (1/1); (c, d) for the cumyl-PNIPAM-MPC (1/5).

The cpa-PNIPAM-MPC (1/12) and the cumyl-PNIPAM-MPC (1/12) have equal size distributions and diameters (see Figure 1d,f and Table 1). Thus, it can be seen that the cumyl- and cpa-RAFT-PNIPAMs have a similar effect in passivating the gold core growth because of their similar molar masses and narrow polydispersities.

The HRTEM images and the size distributions of the cumyl-PNIPAM-MPCs (1/1) and (1/5) prepared through the two-step way are shown in Figure 2. By comparison with the results of PNIPAM-MPCs prepared by the one-step way, it is apparent that the ligands used in the two-step way show much lower effectiveness to passivate the gold core than those used in the one-step way. The mean diameter and the size distribution of the cumyl-PNIPAM-MPC (1/1) (Figure 2 b) are similar to those of the cpa-PNIPAM-MPC (1/5) (Figure 1b) although the former was prepared with a 5-fold higher PNIPAM-SH/$HAuCl_4$ molar ratio than the latter. Also, the size distributions of the cumyl-PNIPAM-MPC (1/5) (Figure 2d) and the cumyl-PNIPAM-MPC (1/12) (Figure 1f) are similar, despite different amounts of the ligands. The two-step way only differs from the one-step way in the PNIPAM ligands. In the two-step way, the cumyl-RAFT-PNIPAM was first hydrolyzed to PNIPAM-SH. The thiol end group is known to react easily and to form disulfide upon exposure to air.[44] In this work, the hydrolysis of RAFT-PNIPAM and the purification of the resulting PNIPAM-SH were carried out under a nitrogen atmosphere. However, two overlapping peaks were observed in the SEC chromatograms: an intense peak related to PNIPAM-SH and a smaller one corresponding to the PNIPAM disulfide with approximately double molar mass. On the other hand, disulfides may be used to passivate the gold core growth as well.[36,45] Therefore, the ligand used in the two-step way is a mixture of the PNIPAM-SH and PNIPAM disulfide and has a broad molar mass distribution compared to the ligands used in the one-step way. This fact probably decreases the effectiveness of mixed ligands, and thus, the size distribution is broad, e.g., for the cumyl-PNIPAM-MPC (1/5) (Figure 2d).

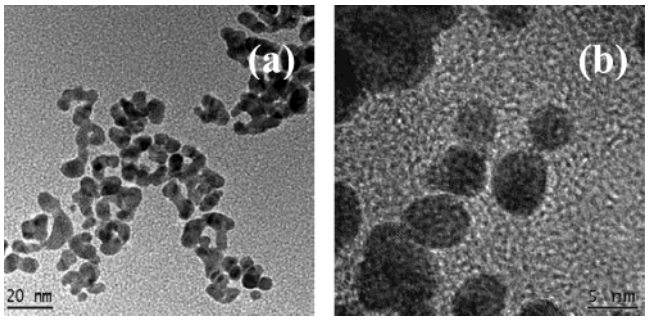

Figure 3. HRTEM images of MPCs prepared by the three-step method: (a) PNIPAM-MPC (1/3) with low magnification; (b) PNIPAM-MPC (1/3) with high magnification.

The HRTEM images of the PNIPAM-MPC (1/3) prepared by the three-step way are shown in Figure 3. The images of PNIPAM-MPC (1/5) are not shown since they are similar to those of the PNIPAM-MPC (1/3). The resulting PNIPAM-MPCs could not be separated in good solvents even using sonication, and it was hard to get an image of the individual nanoparticles by HRTEM (Figure 3a,b). In the three-step way, the PNIPAM-COOH synthesized by conventional radical polymerization has higher polydispersity than RAFT-PNIPAM and probably contains a certain amount of PNIPAM with carboxyl groups at both ends, that is, HOOC-PNIPAM-COOH, and thus forms dithiolated PNIPAM, HS-PNIPAM-SH, during further modification. The fail-

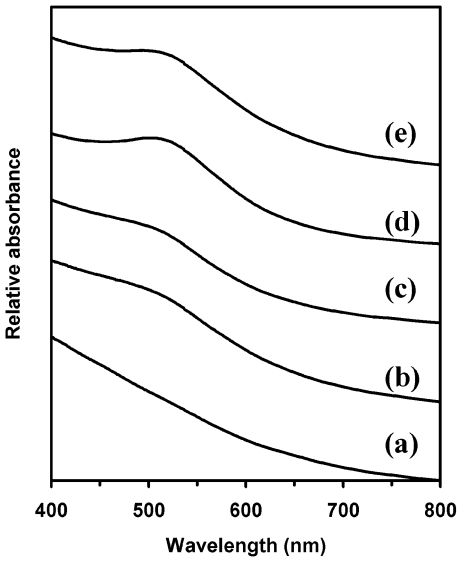

Figure 4. UV−vis spectra of five MPCs in methanol with the gold core size: (a) cumyl-PNIPAM-MPC (1/1), $d = 1.3 \pm 0.4$ nm; (b) cpa-PNIPAM-MPC (1/5), $d = 1.5 \pm 0.5$ nm; (c) cumyl-PNIPAM-MPC (1/5), $d = 2.0 \pm 0.8$ nm; (d) cumyl-PNIPAM-MPC (1/12), $d = 2.2 \pm 0.8$ nm, (e) cpa-PNIPAM-MPC (1/12), $d = 2.3 \pm 0.8$ nm.

ure of the three-step way is attributed to the existence of dithiolated PNIPAM ligands, which bridged the gold clusters together.

As advocated by Whetten,[19,20] the gold cluster shapes were taken as the truncated octahedra in this work. By reference to Murray's work on the alkanethiol-MPCs of gold nanoparticles,[11,14] and according to HRTEM measurements in this work, the gold clusters prepared by the three methods were characterized (Table 1).

Surface Plasmon Bands of PNIPAM-MPCs. The surface plasmon absorption is an optical property for metallic nanoparticles due to the extensive electronic correlation and corresponds to a collective excitation of conduction electrons relative to the ionic core.[46] The intensity of the surface plasmon band (SP band) decreases with decreasing the size of the gold core. Figure 4 shows the dependence of surface plasmon bands for the PNIPAM-MPCs in methanol on the gold core size. The SP band intensity changes with the particle size, but the absorbance maximum is ~518 nm in every case. The SP band becomes undetectable for the smallest particles, the cumyl-PNIPAM-MPC (1/1) (1.3 ± 0.4 nm), which indicates the onset of the quantum size effect. Small particles are regarded to undergo primarily one-electron excitations with a limited amount of electron correlation.[46]

The SP band of nanoparticles is dependent also on the surrounding medium due to the change of the dielectric constant of the medium.[6] In our previous investigation,[34] we found that the aggregation/collapse of PNIPAM layer around the LCST considerably affects the SP band intensity and causes a slight blue shift. In the future, we will further investigate the changes of the optical and optoelectronic properties of the aqueous PNIPAM-MPCs on temperature, pH, and added slat.

The Number of PNIPAM Chains Bound to a Gold Core and the Surface Density. For all of the PNIPAM-MPCs prepared by the methods 1 and 2, the numbers of PNIPAM chains bound to the gold cores were calculated from the thermogravimetric data and are listed in Table 2. For both series of the cumyl- and cpa-PNIPAM-MPCs, the thermal weight loss of PNIPAM fraction measured by TGA decreases with the increasing size of the gold core, while the number of PNIPAM chains bound per gold core increases, this being consistent with the results for alkanethiol-monolayer-protected gold clusters.[11] The two types of RAFT-PNIPAM ligands have similar values of footprints, i.e., ca. 0.40−0.45 nm^2/chain for the cumyl-RAFT-PNIPAM and ca. 0.42−0.54 nm^2/chain for the cpa-RAFT-PNIPAM. If compared with the footprint of PEG-S-ligand (0.35 nm^2/chain, $M_n = 5000$ of PEG-SH) reported by Murray[25] and with the footprint of dodecanethiolate ligand (0.21 nm^2/ligand) reported by Brust,[10,25] it is clear that the PNIPAM ligand is analogous with the PEG-S-ligand to passivate the gold core and more efficient than an alkanethiol.

The surface density of PNIPAM chains for each MPC was calculated in terms of the number of PNIPAM chains bound to a gold core divided by the surface area of the corresponding gold core and ranged from 1.8 to 2.5 chains/nm^2.

Size of PNIPAM-MPCs and Thickness of PNIPAM Monolayer. According to the DLS measurements, most of the PNIPAM-MPCs prepared by methods 1 and 2 even in very dilute aqueous solutions still tend to aggregate. The size distributions were bimodal, representing individual MPCs as well as aggregates. The observed sizes for individual MPCs were close to the estimated values based on the random coil sizes of RAFT-PNIPAM chains, also measured by DLS. The mean hydrodynamic diameters are listed in Table 2.

Table 2. Characterizations of PNIPAM-MPCs and RAFT-PNIPAMs

MPC and PNIPAM	method	wt % PNIPAM[a]	no. PNIPAM chain[b]/ footprint[c]/density[c]	mean diam of MPC or PNIPAM[d] (nm)	thickness of PNIPAM monolayer[e] (nm)
(1) cumyl-PNIPAM-MPC(1/1)	two-step	90	30/0.28/3.6	9.8	4.3
(2) cumyl-PNIPAM-MPC(1/5)	two-step	78	48/0.40/2.5	11.2	4.6
(3) cumyl-PNIPAM-MPC(1/12)	one-step	71	53/0.45/2.2	11.4	4.5
(4) cpa-PNIPAM-MPC(1/5)	one-step	84	26/0.42/2.4	10.0	4.3
(5) cpa-PNIPAM-MPC(1/12)	one-step	68	44/0.54/1.8	12.3	5.0
(6) cumyl-RAFT-PNIPAM				(3.7)	
(7) cpa-RAFT-PNIPAM				3.2 (3.8)	

[a] Thermogravimetric analysis for the thermal loss of PNIPAM fraction. [b] The number of PNIPAM chains bound to per Au core was calculated on the TGA results, combined with the mean size of Au core and the number of Au atoms per core. [c] The footprint of a ligand = the surface area of a gold core/the number of ligands bound to the gold core, nm^2/chain. Note that the footprint is the average value because of the average size of gold core and the average number of ligands. The surface density of PNIPAM chains in the inverse of the footprint, chain/nm^2. [d] For the PNIPAM-MPCs, the mean diameters were determined by DLS in the aqueous solutions; for the cpa-RAFT-PNIPAM, the mean diameters were determined by DLS both in the aqueous solutions and in methanol (corresponding data listed in parentheses), respectively, whereas the mean diameters for the cumyl-RAFT-PNIPAM only was determined in methanol due to its insolubility in water. [e] The thickness of PNIPAM monolayer was the shell thickness, equal to $^1/_2$(the mean diameter of MPC − the mean diameter of gold core).

Scheme 2. Schematic Representation of Cumyl- or Cpa-PNIPAM-MPC and the Thickness of PNIPAM Monolayer Denoted by Arrow

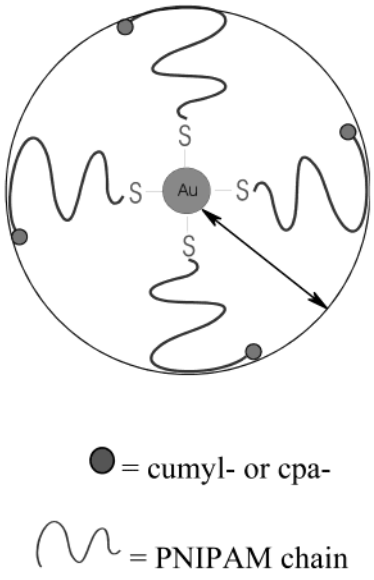

The sizes of the cumyl- and cpa-RAFT-PNIPAM ligands were measured by DLS in methanol and in deionized water, respectively (Table 2). In an aqueous solution of the cpa-RAFT-PNIPAM, DLS measurement showed both the aggregate peak with larger size and the random coil peak with smaller size, and the latter size was taken as the random coil size of cumyl- and cpa-RAFT-PNIPAM.

The thickness of the cumyl- and cpa-PNIPAM monolayers bound to the gold core, calculated from both the MPC sizes and the sizes of the gold cores, is a bit higher than the random coil size of the corresponding cumyl- or cpa-PNIPAM chains (Scheme 2). The difference is small, however, due to the low molar mass of the RAFT-PNIPAM ligands used in this work. On the other hand, the cross-sectional areas of the free RAFT-PNIPAM ligands before binding to the gold cores can be calculated from their random coil sizes in water and in methanol. The values are 10.8 nm^2 for the cumyl-RAFT-PNIPAM (in methanol) and 8.0 or 11.3 nm^2 for the cpa-RAFT-PNIPAM (in water or methanol, respectively). It is evident that the footprints (ca. 0.4 nm^2/chain) of RAFT-PNIPAM chains bound to gold cores are far smaller than the cross-sectional areas of the free RAFT-PNIPAM ligands, but a little larger than the cross-section area (0.1 nm^2) of a sulfur atom (the van der Waals radius of sulfur is 0.18 nm). Therefore, judging from these data and the DLS results, the RAFT-PNIPAM chains bound to the gold cores probably adopt an extended random coil conformation.

Conclusions

By comparing the three methods to prepare gold clusters stabilized by PNIPAM ligands, the one-step way proved most interesting due to the feasibility and the facile control over the sizes of gold clusters with reasonably narrow size distributions. The two types of RAFT-PNIPAM ligands, derived from the RAFT polymerization and directly used in the one-step way, showed higher effectiveness to passivate the gold clusters than the mixed ligands of the PNIPAM-SH and PNIPAM disulfide used in the two-step way. The mixed ligands with a broad molar mass distribution also caused a broad size distribution of MPCs. Using the three-step way, separate gold clusters could not be prepared due to a certain amount of dithiolated PNIPAM as a cross-linking agent.

According to the characterization of gold cores and the analysis of PNIPAM-MPCs prepared by the one-step and two-step ways, the PNIPAM ligand turned out to be a more efficient passivant than alkanethiols; the surface density of PNIPAM chains bound to a gold core was high and ranged from 1.8 to 2.5 chains/nm^2. By combining the DLS data with the footprints of the PNIPAM chains bound to the gold cores and the cross-sectional areas of the free RAFT-PNIPAM ligands, it may be concluded that the PNIPAM chains on the surface of the gold cores are somewhat extended.

Acknowledgment. This work was supported by the Finnish Technology Agency.

References and Notes

(1) McConnell, W. P.; Novak, J. P.; Brousseau, L. C.; Tenent, R. C.; Feldheim, D. L. *J. Phys. Chem. B* **2000**, *104*, 8925−8930.
(2) Niemeyer, C. M. *Angew. Chem., Int. Ed.* **2001**, *40*, 4128−4158.
(3) Shiway, A. N.; Katz, E.; Willner, I. *ChemPhysChem* **2000**, *1*, 18−52.
(4) Remacle, F.; Levine, R. D. *ChemPhysChem* **2001**, *2*, 20−36.
(5) Templeton, A. C.; Wuelfing, W. P.; Murray, R. W. *Acc. Chem. Res.* **2000**, *33*, 27−36.
(6) Kreibig, U.; Vollmer, M. *Optical Properties of Metal Clusters*; Springer Series in Material Science Vol. 25; Springer-Verlag: Berlin, 1995.
(7) Bohren, C. F.; Hoffman, D. R. *Absorption and Scattering of Light by Small Particles*; John Wiley and Sons: New York, 1998.
(8) Taton, T. A.; Lu, G.; Mirtin, C. A. *J. Am. Chem. Soc.* **2001**, *123*, 5164−5165.
(9) Park, S.-J.; Taton, T. A.; Mirtin, C. A. *Science* **2002**, *295*, 1503−1506.
(10) Brust, M.; Walker, M.; Bethell, D.; Schiffrin, D. J.; Whyman, R. *J. Chem. Soc., Chem. Commun.* **1994**, 801−802.
(11) Hostetler, M. J.; Wingate, J. E.; Zhong, C.-Z.; Harris, J. E.; Vachet, R. W.; Clark, M. R.; Londono, J. D.; Green, S. J.; Stokes, J. J.; Wignall, G. D.; Glish, G. L.; Porter, M. D.; Evans, N. D.; Murray, R. W. *Langmuir* **1998**, *14*, 17−30.
(12) Johnson, S. R.; Evans, S. D.; Brydson, R. *Langmuir* **1998**, *14*, 6639−6647.
(13) Porter, L. A., Jr.; Ji, D.; Westcott, S. L.; Graupe, M.; Czernuszewicz, R. S.; Halas, N. J.; Lee, T. R. *Langmuir* **1998**, *14*, 7378−7386.
(14) Templeton, A. C.; Chen, S.; Gross, S. M.; Murray, R. W. *Langmuir* **1999**, *15*, 66−76.
(15) Chen, S.; Kimura, K. *Langmuir* **1999**, *15*, 1075−1082.
(16) Chen, S.; Murray, R. W. *Langmuir* **1999**, *15*, 682−689.
(17) Brust, M.; Fink, J.; Bethell, D.; Schiffrin, D. J.; Kiely, C. *J. Chem. Soc., Chem. Commun.* **1995**, *1655−1656*.
(18) Leff, D. V.; Ohara, P. C.; Heath, J. R.; Gelbart, W. M. *J. Phys. Chem.* **1995**, *99*, 7036−7041.
(19) Whetten, R. L.; Khoury, J. T.; Alvarez, M. M.; Murthy, S.; Vezmar, I.; Wang, Z. L.; Stephen, P. W.; Cleveland, C. L.; Luedtke, W. D.; Landman, U. *Adv. Mater.* **1996**, *5*, 428−433.
(20) Whetten, R. L.; Shafigullin, M. N.; Khoury, J. T.; Schaaff, T. G.; Vezmar, I.; Alvarez, M. M.; Wilkinson, A. *Acc. Chem. Res.* **1999**, *32*, 397−406.
(21) Terrill, R. H.; Postlethwaite, T. A.; Chen, C.-H.; Poon, C.-D.; Terzis, A.; Chen, A.; Hutchison, J. E.; Clark, M. R.; Wignall, G.; Londono, J. D.; Superfine, R.; Falvo, M.; Johnson, C. S., Jr.; Samulski, E. T.; Murray, R. W. *J. Am. Chem. Soc.* **1995**, *117*, 12537−12548.
(22) Hostetler, M. J.; Templeton, A. C.; Murray, R. W. *Langmuir* **1999**, *15*, 3782−3789.
(23) Chen, S.; Ingram, R. S.; Hostetler, M. J.; Pietron, J. J.; Murray, R. W.; Schaaff, T. G.; Alvarez, M. M.; Whetten, R. L. *Science* **1998**, *280*, 2098−2101.
(24) Teranishi, T.; Kiyokawa, I.; Miyake, M. *Adv. Mater.* **1998**, *10*, 596−599.
(25) Wuelfing, W. P.; Gross, S. M.; Miles, D. T.; Murray, R. W. *J. Am. Chem. Soc.* **1998**, *120*, 12696−12697.

(26) Ven Werne, T.; Patten, T. E. *J. Am. Chem. Soc.* **1999**, *121*, 7409−7410.
(27) Mandal, T. K.; Fleming, M. S.; Walt, D. R. *Chem. Mater.* **2000**, *12*, 3481−3487.
(28) Huang, W.; Baker, G. L.; Bruening, M. L. *Angew. Chem., Int. Ed.* **2001**, *40*, 1510−1512.
(29) Huang, W.; Skanth, G.; Baker, G. L. *Lamgmuir* **2001**, *17*, 1731−1736.
(30) Jordan, R.; West, N.; Ulman, A.; Chou, Y.-M.; Nuyken, O. *Macromolecules* **2001**, *34*, 1606−1611.
(31) Ohno, K.; Koh, K.-m.; Tsujii, Y.; Fukuda, T. *Macromolecules* **2002**, *35*, 8989−8993.
(32) Mandal, T. K.; Fleming, M. S.; Walt, D. R. *Nano Lett.* **2002**, *2*, 3−7.
(33) Nuss, S.; Böttcher, H.; Wurm, H.; Hallensleben, M. L. *Angew. Chem., Int. Ed.* **2001**, *40*, 4016−4018.
(34) Raula, J.; Shan, J.; Nuopponen, M.; Niskanen, A.; Jiang, H.; Kauppinen, E.; Tenhu, H. *Langmuir* **2003**, *19*, 3499−3504.
(35) Corbierre, M. K.; Cameron, N. S.; Sutton, M.; Mochrie, S. G. J.; Lurio, L. B.; Ruhm, A.; Lennox, R. B. *J. Am. Chem. Soc.* **2001**, *123*, 10411−10412.
(36) Mangeney, C.; Ferrage, F.; Aujard, I.; Marchi-Artznern, V.; Jullien, L.; Ouari, O.; Rekai, E. D.; Laschewsky, A.; Vikholm, I.; Sadowski, J. W. *J. Am. Chem. Soc.* **2002**, *124*, 5811.
(37) Lowe, A. B.; Sumerlin, B. S.; Donovan, M. S.; McCormick, C. L. *J. Am. Chem. Soc.* **2002**, *124*, 11562−11563.
(38) Mitsukami, Y.; Donovan, M. S.; Lowe, A. B.; McCormick, C. L. *Macromolecules* **2001**, *34*, 2248−2256.
(39) Thang, S. H.; Chong, Y. K.; Mayadunne, R. T. A.; Moad, G.; Rizzardo, E. *Tetrahedron Lett.* **1999**, *40*, 2435−2438.
(40) Ganachaud, F.; Monteiro, M. J.; Gilbert, R. G.; Dourges, M.-A.; Thang, S. H.; Rizzardo, E. *Macromolecules* **2000**, *33*, 6738−6745.
(41) Bernkop-Schnurch, A.; Kast, C. E.; Richter, M. F. *J. Controlled Release* **2001**, *71*, 277−285.
(42) Bernkop-Schnurch, A.; Scholler, S.; Biebel, R. G. *J. Controlled Release* **2000**, *66*, 39−48.
(43) Yee, C. K.; Jordan, R.; Ulman, A.; White, H.; King, A.; Rafailovich, M.; Sokolov, J. *Langmuir* **1999**, *15*, 3486−3491.
(44) Kato, K.; Ito-Akita, K.; Ohno, H. *J. Solid State Electrochem.* **2000**, *4*, 141−145.
(45) Porter, L. A.; Ji, D.; Westcott, S. L.; Graupe, M.; Czernuszewicz, R. S.; Halea, N. J.; Lee, T. R. *Langmuir* **1998**, *14*, 7378−7386.
(46) Johnston, R. L. *Atomic and Molecular Clusters*; Taylor & Francis: London, 2002.

MA034265K